Experimental investigation of the effect of a B70 biodiesel blend on a common-rail passenger car diesel engine

D Tziourtzioumis, L Demetriades, O Zogou, and **A M Stamatelos***
Laboratory of Thermodynamics and Thermal Engines, Department of Mechanical and Industrial Engineering, University of Thessaly, Volos, Greece

The manuscript was received on 12 December 2008 and was accepted after revision for publication on 9 February 2009.

DOI: 10.1243/09544070JAUTO1094

Abstract: The results of engine bench tests of a 2.0 l common-rail high-pressure injection passenger car diesel engine fuelled by B70 biodiesel blend are compared with the corresponding results of baseline tests with standard EN 590 diesel fuel. Engine performance and carbon monoxide (CO), total hydrocarbon, and nitrogen oxide NO_x emissions were measured. Also, indicative particulate sampling was made with a simplified undiluted exhaust sampler. The aim of this study was to understand better how the engine's electronic control unit (ECU) responds to the different fuel qualities. A series of characteristic operation points for engine testing is selected to serve this purpose better. Data acquisition of the engine ECU variables was made through INCA software. Also, additional data acquisition based on external sensors was carried out by means of Labview software. The results enhance our understanding of the engine ECU behaviour with the B70 biodiesel blend. Also, they are compared with what is known from the related literature for the behaviour of common-rail diesel engines with biodiesel blends.

Keywords: BFO biodiesel blend, common-rail diesel engine, passenger cars, engine bench tests

1 INTRODUCTION

According to the ambitious report of the Biofuels Research Advisory Council [**1**], the European Union could replace 25 per cent of its transportation fuels by biofuels by 2030. Owing to the specific fuel balances existing in the European fleet, which make Europe a net exporter of gasoline and importer of diesel fuel, it is estimated that this target would be most probably realized mainly by biodiesel (75 per cent biodiesel versus 25 per cent bioethanol) [**2**]. In Greece, biodiesel, in the form of fatty acid methyl esters (FAMEs), has been produced since 2005 and is currently mixed in the diesel fuel at about 4 vol %, this percentage being slowly but steadily increasing. The production capacity of existing biodiesel factories in Greece can supply the required quantities to increase the biodiesel blending percentage to up to 15 per cent, provided that the necessary vegetable oil and recycled oil quantities will become available and prices be favourable. According to Greek legislation, at least 30 per cent of the raw material must be domestically produced. Nowadays, automotive manufacturers allow running of modern diesel-powered passenger cars on blends of biodiesel up to B30, provided that certain additional maintenance measures are taken, including more frequent fuel and oil filter changes, together with inspection of engine oil level and the fuel lines and injection system components for possible leaks. In order to ensure customer's acceptance, standardization and quality assurance are key factors for the market introduction of biodiesel as a transport fuel.

According to a common statement by the diesel fuel injection systems manufacturer's association

**Corresponding author: Laboratory of Thermodynamics and Thermal Engines, University of Thessaly, Department of Mechanical and Industrial Engineering, Pedion Areos, Volos, 383 34, Greece. email: stam@uth.gr*

[**3**], diesel fuel specifications (EN 590 in Europe, and D6751 in the USA) should be regularly updated to allow for the gradually increasing percentage of biodiesel mixing (currently 5 per cent but soon to be extended to 7 per cent + 3 per cent). In this way, the injection system's components are to be protected from possible secondary effects of FAMEs which include fuel leakage or filter plugging due to the softening, swelling or hardening, and cracking of some elastomers and displacement of deposits from diesel operation, corrosion of aluminium or zinc parts in fuel injection equipment due to free methanol residues, filter plugging or corrosion of fuel injection equipment due to residues of the FAME process chemicals, corrosion of fuel injection equipment or filter plugging due to the hydrolysis of FAME by free water residues (bacterial growth), filter plugging or injector coking due to corrosion of non-ferrous metals by free glycerine residues, filter plugging because of lacquer formation by soluble polymers in hot areas due to the precipitation of deposits, and generation of excessive local heat in rotary distributor or supply pumps due to the high viscosity of the biodiesel [**4**]. Also, further oxidation stability improvements are considered essential to increase the biodiesel blending percentages above 20 per cent. Resistance to oxidative degradation during storage is an increasingly important issue for biodiesel [**5**, **6**].

The effects of biodiesel blends on the operation, performance, and emissions of diesel engines have been studied in a vast amount of published and unpublished research work, since 1980 [**4**, **7**, **8**]. The combustion of biodiesel in engines equipped with pump–line–nozzle fuel systems normally results in advancement of the start of injection and combustion, due to the differences in chemical and physical properties of the fuels. Unit injector or common-rail injection-system-equipped engines do not exhibit the same behaviour [**9**, **10**].

As a general trend, the combustion of biodiesel blends reduces carbon monoxide (CO), hydrocarbon (HC), and particulate emissions, in both older technology and modern diesel engines, depending also on the specific quality of biodiesel employed [**11**]. In addition to legislated pollutants, biodiesel is known to reduce several unregulated pollutant species significantly.

In this paper, an attempt is made to understand better how the engine's electronic control unit (ECU) operates with a high biodiesel (FAME) blend in modern common-rail injection diesel engines, and thus to explain the observed effects on the engine performance and emissions characteristics. The results are compared with what is reported in the specialized literature for the specific engine category and high blending rates [**12**, **13**].

2 THE EVOLUTION TO THE COMMON-RAIL DIESEL INJECTION SYSTEMS

The variety of reported trends in the effect of biodiesel fuel blends on diesel engine combustion can be mainly attributed to the variety of existing, older, and modern fuel injection systems, especially for passenger car diesels. Starting from the pre-chamber and swirl-chamber engines where the combustion was initiated in rich blend conditions in the prechamber and continued later in the main chamber, where the partially burned blend was injected, equipped with glow plugs for the preheating of the prechamber and rotary-type fuel pumps, which distribute at 130–150 bar the fuel to the pressure-operated injectors, with the increased particulate emissions in transient operation, technology shifted during the 1990s to the direct-injection (DI) diesel engines, with a distributor pump with increased injection pressure levels (180–250 bar) and some electronic parts. Thus, the passenger diesel cars acquired the well-known fuel economy, reliability, lower cylinder head thermal loading, lack of preheaters, etc., advantages of the DI engines traditionally employed in trucks and buses. However, they also had their disadvantages, such as the increased noise levels, and the difficulties to attain the increasingly stringent particulate and nitrogen oxide (NO_x) emissions standards.

Modern passenger car diesel engines are of the common-rail high-pressure DI technology. A rotary pump supplies a common rail with high pressure (1300–2000 bar) fuel. The injectors are fed by this rail, controlled by an electric valve, based on ECU signals. These engines are quieter and cleaner as regards emissions, especially during acceleration, owing to the improved control of combustion, by means of dividing injection into pilot injection, main injection, and possibly post-injection, when necessary for exhaust temperature increase to induce regeneration of the diesel filter.

Diesel engine emissions are known to be affected by the fuel quality, engine operation temperature, combustion chamber type and technology, fuel injection system technology, engine operation point, and operation conditions. During the last 15 years, engine exhaust emission standards in Europe, measured according to the New European Driving

Cycle (NEDC), evolved from Euro 1 (1993: CO, less than 3.16 g/km; $HC+NO_x$, less than 1.13 g/km; particulate, less than 0.16 g/km) to Euro 4 (2006: CO, less than 0.5 g/km; $HC+NO_x$, less than 0.56 g/km; NO_x, less than 0.25 g/km particulate, less than 0.025 g/km) and beyond. In particular the NO_x and particulate standards are extremely stringent; the latter require the use of a particulate filter as standard equipment in modern diesel passenger cars.

Fuel quality standards, on the other hand, have a gradually diminishing sulphur content (e.g. for EN-590, in 1996, 0.05 per cent; in 2005, 50 ppm; in 2009, 10 ppm). Also, they have a generally increasing cetane index and allow the use of additives assisting emissions reduction.

The injection pressure in common-rail systems can be controlled irrespective of engine speed and stays constant during the injection phase. The accurate control of injector opening and closing by a microcomputer allows for a wide range of possibilities for tailoring the injection and combustion curve by the engine manufacturer. The injected fuel quantity can be divided into separate parts, namely the pilot injection which reduces engine noise due to self-ignition of the initial injected quantity, as well as the NO_x formation. This small quantity of fuel (1–4 mm^3) allows for a more regular combustion, with gradual increases in temperature and pressure in the combustion chamber. The microcomputer control of all injection parameters, based on previously defined maps that are saved in the ECU memory, allow the optimization of steady state and transient engine operation.

The high-pressure pump has been designed to supply significant fuel quantities with respect to the engine needs. The surplus quantity returns to the tank by means of a leak orifice that is controlled by the pressure regulator. The pressure regulator controls the rail pressure, based on the engine speed and load. The required pressure value is computed by the ECU and confirmed on the basis of the information fed back by the rail pressure sensor. The rail pressure varies between 280 bar (low load) and 1400 bar (high load), or even more, up to 2000 bar [**14**].

The injection pressure control loop is based on the determination, by the ECU, based on the engine speed and load, of the target value of the injection pressure. This value is fed to the pressure regulator. The actual rail pressure is fed back to the ECU to complete the control loop. The activation time of the injector solenoid valve varies between 200 μs and 1200 μs.

In contrast with older injection systems, the ECU determines independently the injected fuel quantity and injection advance. The injected fuel quantity is determined by the ECU, by means of a combination of rail pressure and injection duration. The regulation of the fuel quantity is based on the estimation by the ECU, based on the respective sensors' signals and the rail pressure signal and the respective maps, of the required fuel quantity and the respective duration of injectors' current.

The rail pressure significantly affects the injected fuel quantity per degree crank angle (CA), as well as the degree of atomization of the fuel. The injector opening duration, the injector needle lift and the number and diameter of injection orifices are the main factors determining the fuel delivery per stroke.

The engine ECU takes into account the following sensor's signals:

(a) the throttle position;
(b) the cooling water temperature;
(c) the fuel temperature;
(d) the engine speed and crankshaft position;
(e) the ambient absolute pressure and intake manifold pressure;
(f) the vehicle speed;
(g) activation of braking and clutch decoupling contact;
(h) the intake air mass flowrate and temperature;
(i) the exhaust gas recirculation (EGR) valve position
(j) the compressor boost pressure.

The ECU takes additionally into account the respective engine operating mode, i.e. engine start-up (additional fuel delivery for start-up), engine idle (idle fuel flowrate), normal operation, cold start, acceleration fuel enrichment, etc.

An important sensor for the operation with biodiesel fuel blends is the fuel temperature sensor, normally of the CTN™ type, usually placed on the rail or on the fuel return circuit. This sensor's signal allows the ECU to correct the injected fuel quantity, to make up for the fuel viscosity decrease with increasing temperature.

3 LITERATURE REVIEW: COMMON-RAIL DIESEL ENGINES WITH BIODIESEL

Rapeseed biodiesel has been in use in Germany since the early 1980s. Its use has been progressively increasing in Europe and North America during the

subsequent years. An initial review of the related literature, published in reference [**7**], soon became obsolete. The last decade was marked by an impressive expansion of international interest on biofuels, supported by a highly ambitious position by the European Union [**1**, **15**]. However, a certain slowdown in the expansion of the use of biofuels has been observed recently, which is due to scepticism about possible side effects on the prices of foodstuff, as well as the need to study the plant- to- wheel efficiency and sustainability of biofuel production and use better. Despite the slower increase in biofuels penetration in the market, the specialized research literature is expanding at an ever-increasing rate.

An inclusive literature review on the general subject of the effect of biodiesel on engine performance and emissions, which covers more recent work done during the last decade, has been presented in reference [**8**]. As regards the effects of biodiesel blends on CO and total hydrocarbon (THC) emissions, most researchers have reported a sharp decrease when substituting conventional diesel fuel with biodiesel fuels. A review by the US Environmental Protection Agency (EPA) [**16**] indicated a 70 per cent mean reduction in THC levels and about 50 per cent in CO when the engine is fuelled by pure biodiesel instead of conventional diesel. The reasons proposed to explain this decrease include the oxygen content of the biodiesel, the higher cetane number of biodiesel reducing combustion delay, the higher final distillation point of diesel fuel (THC emissions), the advanced injection, and combustion timing. Nevertheless, it will be necessary to carry out significant research work with modern common-rail diesel engines in order to understand the effects of biodiesel blends on the injection, combustion, and emissions of ultra-low emitting engines better. In particular, with the EURO 4 engines equipped with diesel particulate filters, which are now on the European market, it will be necessary to study in depth the effect of biodiesel on the operation of the different filter and regeneration technologies and engine durability effects due to oil dilution from post-injection.

NO_x and particulate matter (PM) emissions are the main concern for modern diesel engines, owing to the high-temperature lean diffusion flame of the diesel combustion chamber. NO_x and PM emissions of modern diesel engines are very close to the legislated standards, which are becoming increasingly stringent. For example, EURO 5 legislation is expected to reduce NO_x and PM emissions of passenger cars from 0.25 g/km and 0.025 g/km of today to 0.18 g/km and 0.005 g/km respectively in the NEDC [**17**]. Moreover, EURO 5 legislation may additionally check particulate number and not only mass, provided that a commonly accepted methodology and measurement device is agreed upon [**18**]. An improved understanding of the pollution reduction potential of biodiesel in modern diesel engines would help car manufacturers to adapt their engines better to the use of higher percentages of biodiesel, compromising between efficiency and cost. Also, it would help local authorities to promote biodiesel use further in urban areas with a high percentage of diesel-powered vehicles as a means of improving air quality.

3.1 Engine power and efficiency

Biodiesel presents a reduced gross heating value compared with diesel fuel (see Table 1 later). This holds true also per unit volume and results in higher volume fuel consumption whenever diesel fuel is substituted by biodiesel. Thus, when the engine is tested on the test bench, maximum power is reduced unless the fuel pump maximum fuel delivery per stroke is increased to compensate for the lower heating value reduction. Although the reported rated

Table 1 Comparison of the range of variation in the main fuel properties, between biodiesel and diesel fuel. Properties of the specific fuels employed in this study are also included in the last two columns.

	Value for the following			
Parameter (units)	Biodiesel (range)	Diesel (range)	This case, Biodiesel (FAME)	This case, Diesel
Density (15 °C) (kg/m^3)	860–895	815–845	865	825
Viscosity (40 °C) (cSt)	3.5–5.5	2–3.5	4.7	2.5
Cetane number	45–65	40–55	55	50
Cold filter plugging point (°C)	−5 to 10	−25 to 0	−3	−12
Gross heating value (MJ/kg)			40.3	46.1
Lower heating value (MJ/kg)	36.5–38	42.5–44	37.7	43.3
Water content (mg/kg)	0–500		330	–
Acid number (mg KOH/g)	0–0.60		0.16	–
Sulphur content (ppm)		10–500		50
Iodine number (g iodine/100 g)			117	–

power reduction is about 8 per cent for B100 and, by analogy to lower blends, there exist some variation around this percentage among different engines and researchers [**19**–**23**]. In older injection systems, the higher viscosity, which reduces the back flow across the piston clearance of the injection pump, may further compensate the loss in heating value. In addition, the higher bulk modulus and sound velocity of biodiesel [**24**–**26**], together with its higher viscosity [**27**], lead to an advanced start of injection. This, jointly with the cetane number increase, may slightly advance the start of combustion, which sometimes may increase the power output.

The engine thermal efficiency, as calculated from brake specific fuel consumption (bsfc), is employed to compare the performances of different fuels, besides their heating value. Most researchers observed no significant change in thermal efficiency when using biodiesel [**8**, **28**]. However, the thermal efficiency with alternative fuels should always be calculated with the necessary accuracy; i.e. the heating value of the fuel must be measured, together with the fuel density, in the case of volumetric fuel flowrate measurement. The fuel density changes with temperature should also be taken into account [**29**].

3.2 NO_x emissions

Most of the literature reviewed in reference [**8**] showed either a slight NO_x emissions increase with biodiesel blends, or no important effect at all. The increase in NO_x in older-technology engines is mainly attributed to the advancement in injection derived from the physical properties of biodiesel (viscosity, density, compressibility, and speed of sound). The effect of the physical properties of biodiesel on the injection advance (with respect to the start of injection with diesel fuel) has been widely proved in older-technology engines. When biodiesel is injected, the pressure rise produced by the pump propagates more quickly towards the injectors because of its higher sound velocity. In addition, the higher viscosity reduces leakages in the pump, leading to an increase in the injection line pressure. Therefore, a quicker and earlier needle opening is observed with respect to diesel fuel.

Nowadays, the injection cartographies are optimized by engine designers as a function of the NO_x–soot trade-off [**8**]. Delaying injection can reduce the NO_x emissions level, increasing of course the PM emissions [**14**]. Leung *et al.* [**30**] proposed that other injection parameters, in combination with injection timing, should be modified in order to eliminate the expected NO_x emissions increase without any penalty in PM reductions.

The effect of the increased oxygen availability on NO_x emissions has also been examined. Lapuerta *et al.* [**8**] concluded that the oxygen content of biodiesel could not cause any increase in NO formation because diffusion combustion occurs mainly in regions with the oxygen-to-fuel ratio around stoichiometric, which is 2.81 for biodiesel and 3.58 for a standard diesel fuel. They argued that internal oxygen in the fuel molecule is not enough to compensate this difference.

3.3 Particulate matter and smoke opacity

The literature search made in reference [**8**] concluded that almost the majority of researchers reported a noticeable decrease in PM emissions with the use of biodiesel blends as fuel. However, this reduction in the solid fraction of the particulate is accompanied by an increase in the soluble organic fraction (SOF). Such an increase could be due to the lower volatility of the unburned HCs from biodiesel combustion, which favours their condensation and adsorption on the particles surface. Yamane *et al.* [**31**] carried out optical visualizations of the fuel jet and found that evaporation and air mixing are slower with biodiesel. The following factors are reported to explain the particulate reduction by use of biodiesel: the oxygen content of the biodiesel molecule, which promotes combustion even in fuel-rich regions, the lower stoichiometric air-to-fuel ratio $(A/F)_{st}$ of biodiesel combustion, which reduces the probability of fuel-rich regions. Also, the non-existence of aromatics in biodiesel fuels and the zero sulphur content of most biodiesel fuels, which prevents sulphate formation. Finally, it is known that biodiesel, despite its higher average distillation temperature, demonstrates a lower final boiling point; i.e. heavy distillates that are unavoidably present in small quantities in diesel fuel are absent in biodiesel because of its natural origin. The absence of such heavy HCs unable to vaporize (soot precursors) reduces soot emissions [**8**, **32**, **33**].

4 PROPERTIES OF TESTED FUELS

The fuels under investigation are pure diesel (0 per cent biodiesel), and a blend of 70 vol % biodiesel in pure diesel. Throughout this paper the tested fuels were denoted as B0 and B70 respectively. B0

conforms to European standard EN 590. The biodiesel employed in the measurements is an FAME produced by 40 per cent rapeseed oil, 30 per cent soybean oil, and 30 per cent recycled cooking oils. It was supplied by ELIN biofuels SA (Volos factory) and conforms to EN 14214:2003 specifications [**34**]. A comparison between the tested fuels is given in Table 1, together with the corresponding range of variation in each parameter for the different fuel types used in Europe and North America [**35**, **36**]. Unfortunately, the exact methyl esters profile of the tested biodiesel was not available. However, since the fatty acid profile of biodiesel is identical with that of the parent oil, an approximate profile corresponding to the above parent oil mixing percentages can be estimated on the basis of the indicative methyl esters profiles discussed in reference [**37**]. Based on the additional assumption that the recycled cooking oils are composed of sunflower and palm oil, an approximate methyl ester profile was estimated to consist of 12 per cent C16:0, 5 per cent C18:0, 40 per cent C18:1, 36 per cent C18:2, and 7 per cent C18:3. Based on this profile, $(A/F)_{st}$ for the pure biodiesel is calculated to 12.48.

5 TEST EQUIPMENT AND PROCEDURE

The experimental work [**38**] was made on a PSA 2.0 L, four-cylinder, four-stroke turbocharged intercooled common-rail DI light-duty diesel engine connected to a Froude–Consine eddy current dynamometer with Texcel 100 direct digital controller and a PWM engine throttle actuator. The main specifications of the engine are given in Table 2. The engine is equipped with a Bosch common-rail fuel injection system which enables up to three injections per cycle and provides a 1350 bar maximum rail pressure. The injection system parameters and EGR are controlled via the ECU. The ETAS/MAC 2 interface and the INCA software interface were used for the data acquisition of the engine ECU variables.

Table 2 Engine technical data

Engine type	High-pressure turbocharged engine
Engine model	DW10 ATED
Cylinders	4, in line
Bore	85 mm
Stroke	88 mm
Displacement	1997 cm^3
Rated power	80 kW, 4000 r/min
Rated torque	250 N/m, 2000 r/min
Compression ratio	18:1
ECU version	Bosch EDC 15C2 HDI
Diesel filter	IBIDEN SiC filter

Also, additional data acquisition based on external sensors was carried out by means of an NI Data acquisition cards and Labview software. These include pressures (by piezoresistive transducers) and temperatures (by K-type thermocouples) at various points along the engine inlet and exhaust line, fuel and air flowrates; and the air-to-fuel ratio (A/F) for control purposes by means of a universal exhaust gas oxygen (UEGO) sensor. Sampling of exhaust gas is led to a pair of THC analysers (JUM HFID 3300A), CO, carbon dioxide (CO_2) (signal model 2200 non-dispersive infrared detector) and NO_x (signal model 4000 chemoluminescence detector) analysers.

5.1 Basic fuel injection maps

In order to understand the variation in the specific engine's behaviour with biodiesel blends better, the mapping of the basic injection parameters in the engine's ECU is to be discussed first. The main maps that are stored in the ECU are summarized below (Fig. 1). They are employed in the calculation of the following variables:

(a) the common-rail pressure as a function of the engine speed and fuel delivery per stroke (Fig. 2);
(b) the injector opening duration (μs) as a function of the rail pressure and fuel delivery per stroke (The injection system enables up to three injections per cycle to be made, namely pilot, main, and post injection (Fig. 3);
(c) the pilot injection fuel delivery (mm^3/stroke) as a function of the engine speed and total fuel delivery (Fig. 4);
(d) the pilot injection advance (°CA) as a function of the engine speed and fuel delivery per stroke (Fig. 5);
(e) the main injection advance (°CA) (with pilot injection) as a function of the engine speed and fuel delivery per stroke (Fig. 6).

Data acquisition of the engine's ECU variables was made through INCA software, which may record several hundreds of ECU variables. The following variables were regularly recorded (with a time step of 100 ms) during our measurements: the engine speed, pedal position, water temperature, EGR valve position, throttle valve position, turbo valve position, intake air temperature, intake pressure (set point and measured), air mass flow (set point and measured), fuel temperature, fuel pressure (set point and measured), fuel mass delivery per cycle, injec-

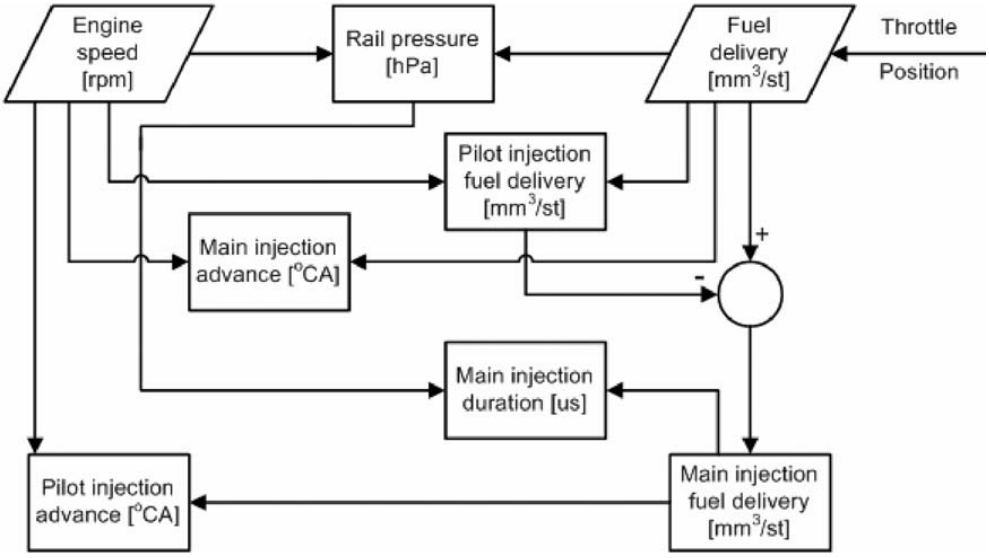

Fig. 1 ECU flow chart for the calculation of the main injection parameters (common-rail injection system)

tion advance (pilot), injection advance (main), and injection duration (pilot, main, and post injection).

Also, additional data acquisition based on external sensors was carried out by means of Labview software and was made for the following quantities: the engine speed, engine torque, cooling water inlet and outlet temperatures, fuel mass flowrate, air flowrate, A/F, compressor boost pressure, turbo in pressure, and temperatures and pressures at various points in the engine inlet and exhaust lines, including the oxidation catalyst and diesel filter.

A succession of steady state operation points was selected as shown in Fig. 7. The set of operation points was selected to cover the full extent of the engine operation map (from low speed and low load to high speed and high load) and thus to study also engine operation that is not represented in the legislated cycles (e.g. NEDC), which usually focus on the lower left quadrant of the speed – load regime. The specific sequence of operation points was programmed in the dyno controller (test sequence

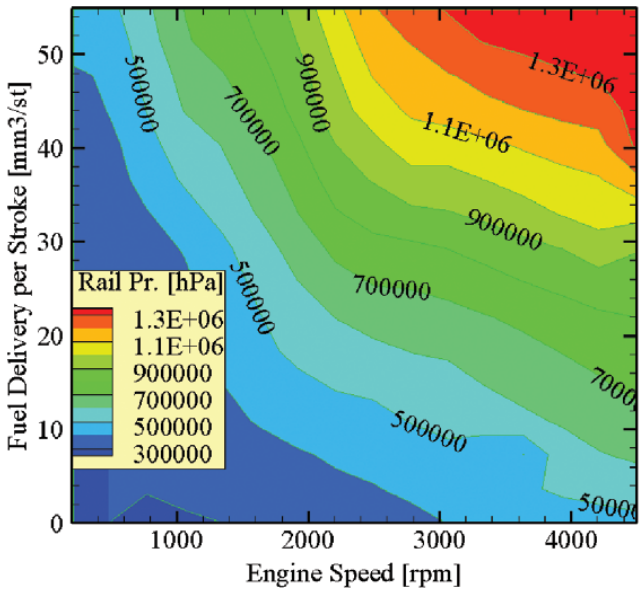

Fig. 2 Common-rail pressure as a function of engine speed and fuel delivery per stroke

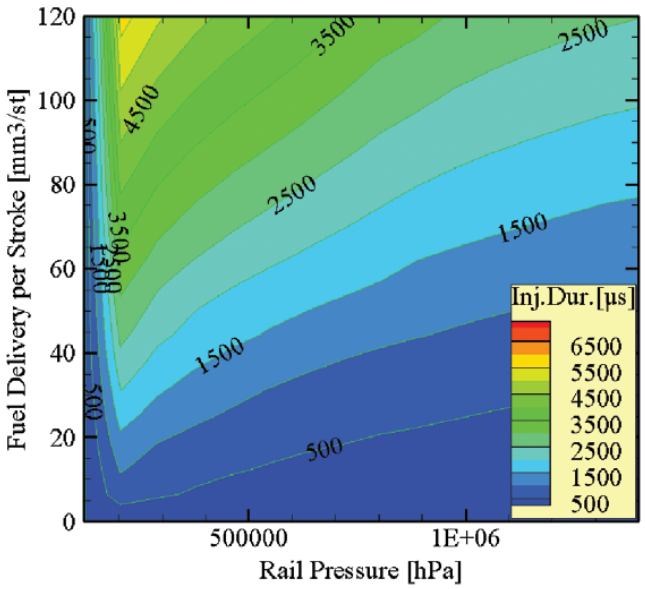

Fig. 3 Injector opening duration as a function of rail pressure and fuel delivery per stroke (pilot, main, and post injection)

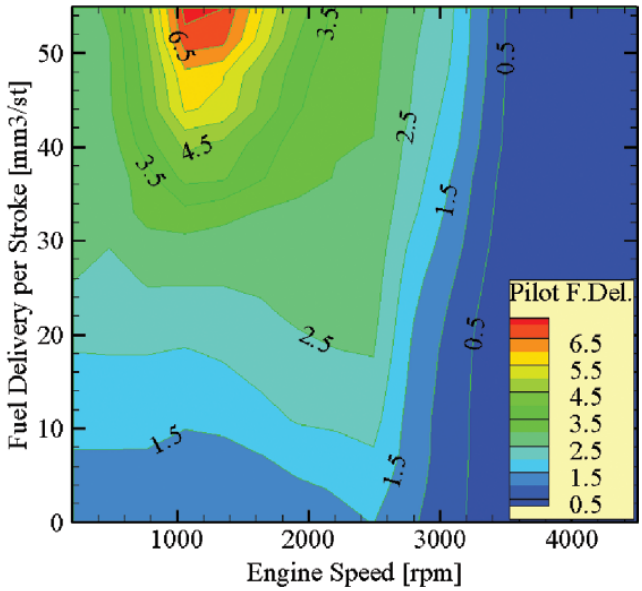

Fig. 4 Pilot injection fuel delivery (μs) as a function of the engine speed and total fuel delivery

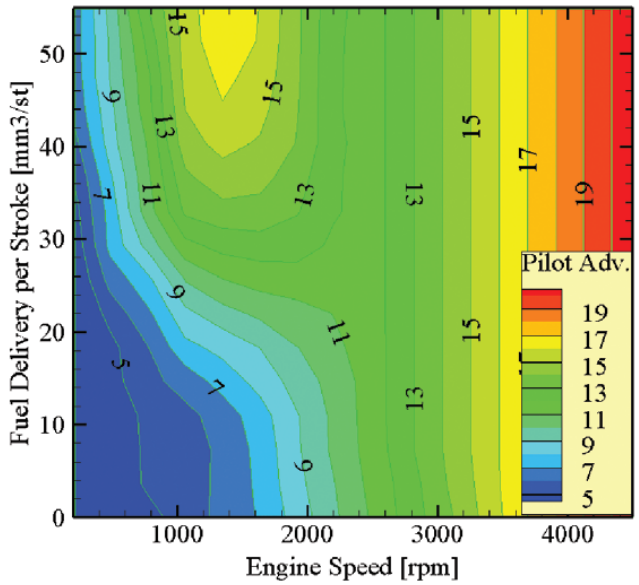

Fig. 5 Pilot injection advance (°CA) as a function of the engine speed and fuel delivery per stroke

editor). The transition time between each two successive points was set to 5 s.

As regards secondary effects of the use of the B70 biodiesel blend, during the tests with B70, fuel leaks due to the loosening of the fitting of the elastic pipe which leads fuel returns to the fuel tank were noticed. Additionally, high fuel temperatures were measured in the fuel return line, and a counter-flow heat exchanger (water-to-fuel) had to be installed for return line cooling, by means of 20 °C water from the supply. This effect has already been reported by

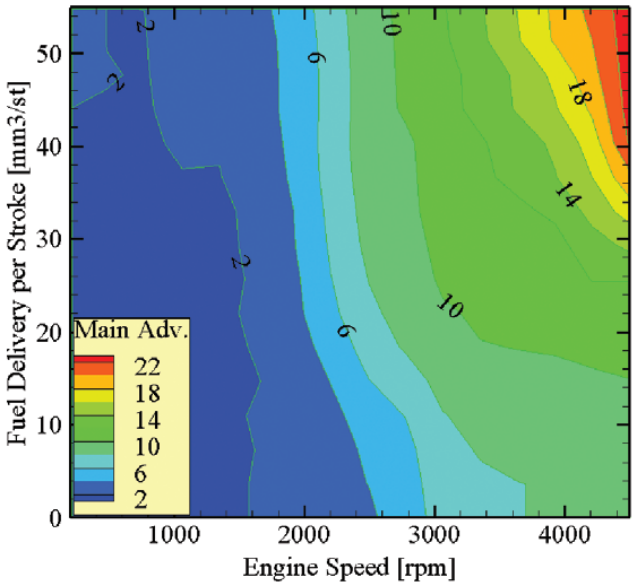

Fig. 6 Main injection advance (°CA) (with pilot injection) as a function of the engine speed and fuel delivery per stroke

other researchers with injection systems based on a rotary supply or distributor pumps [**4**].

6 RESULTS AND DISCUSSION

6.1 Effect of B70 on engine performance and fuel consumption

As already reported in section 5, the dyno controller was programmed to attain the same operation points for both alternative fuels used. However, the real engine performance was slightly affected as shown in Fig. 8. Small differences in engine torque are observed, which fall within the statistical variability of engine performance. The results are presented below in the form of line graphs, where the horizontal axis contains always the numbers of the 15 operation points of the sequence of Fig. 7. Thus, the lines connecting the 15 values of each variable in the graphs are not representing any intermediate operation points. They are just connecting the points to allow the simultaneous presentation of the variation in more related variables in one graph, which could not easily be achieved with a bar chart.

The most marked difference in the performance of the engine fuelled by B70 is the increase in fuel delivery per stroke, for the respective operation points, as presented in Fig. 9. There exists only one operation point where a decrease in fuel consumption with B70 is observed. This could be possibly due

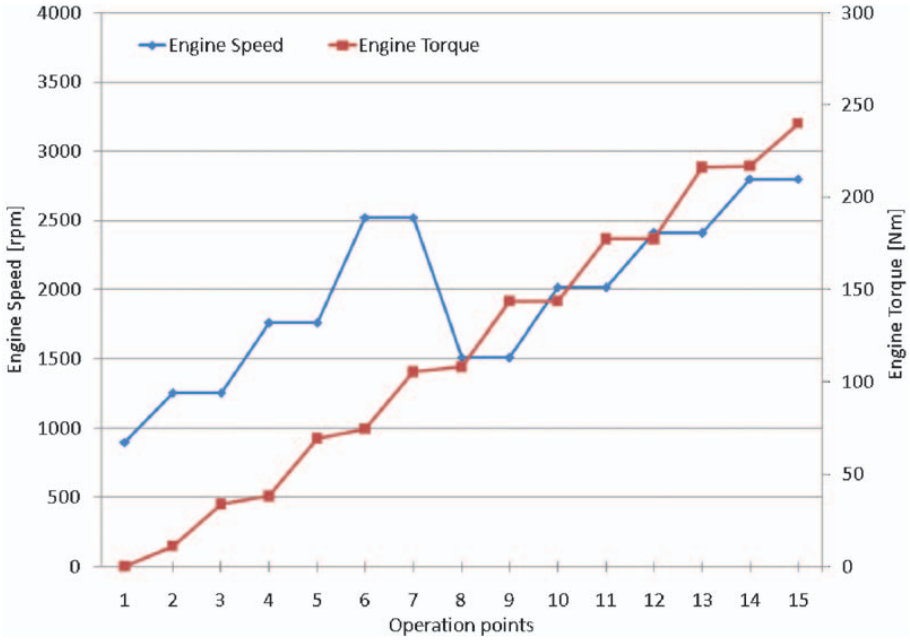

Fig. 7 Sequence of operation points selected for the comparison of fuels

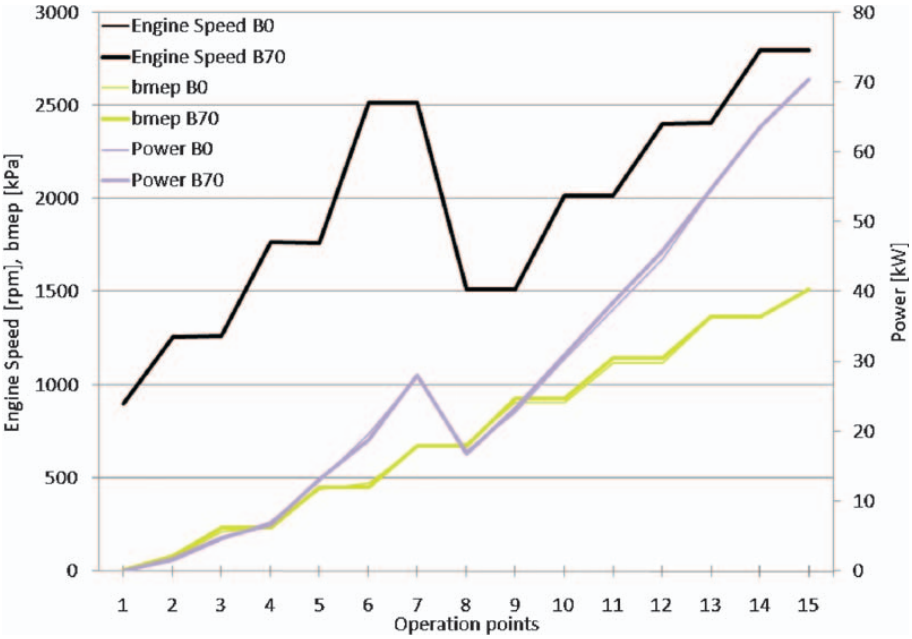

Fig. 8 Comparison of the engine speed, brake mean effective power (bmep), power with Diesel fuel and B70 blend at the 15 operation points of the cycle

to a significant difference in engine efficiency and turbocharger speed at this low-load operation point with EGR.

The increase in fuel delivery per stroke is expected, as already mentioned. Additional fuel mass is required in order to produce the same power per cycle burning a blend with lower heating value (Table 3). Gross heating value of the two fuels was measured in a Parr 1261 oxygen bomb. The results are presented in Table 3.

According to the results in Table 3, the lower heating value of the B70 blend is 37.7 MJ/kg, whereas the corresponding value for the diesel fuel is 43.3 MJ/kg.

In order to calculate the fuel energy input per stroke, it is necessary additionally to take into

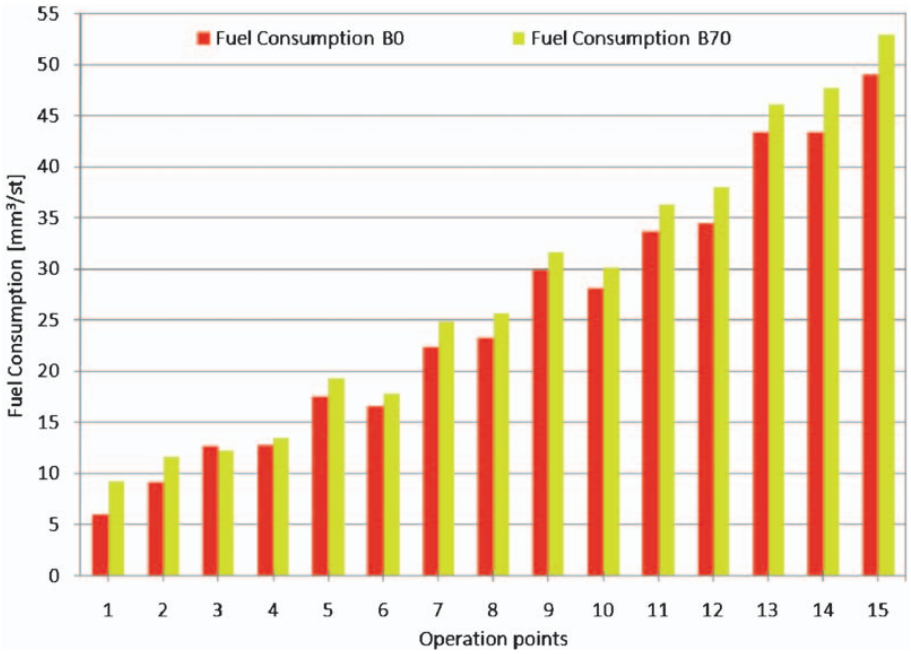

Fig. 9 Fuel consumption b_{sp} increase with B70 versus diesel fuel at the 15 operation points of the cycle

Table 3 Results of Gross heating value measurements with the bomb calorimeter

	Gross heating value (MJ/kg)	Mean gross heating value (MJ/kg)	Mass of H_2O in the exhaust gas per kg of fuel	Lower heating value (computed) (MJ/kg)
Diesel EN 590				
1	46.0434	46.2276	1.17	43.30
2	46.2124			
3	46.4261			
Biodiesel EN 14214				
1	40.1051	40.2913	1.04	37.69
2	40.4928			
3	40.2761			

account the fuel density, which is also a function of fuel temperature according to

$$\rho_f = \frac{\rho_0}{(1+\beta\,\Delta t)} \tag{1}$$

The coefficient of thermal expansion of biodiesel is assumed to be $\beta = 8.3\times10^{-4}$ [**39**]. The coefficient of thermal expansion of diesel fuel is assumed to be $\beta = 11\times10^{-4}$ [**40**], and ρ_0 is the reference density at 15 °C (Table 1).

Based on the above, the fuel energy input per stroke is given by the equation

$$E_{str} = \rho_f H_u b_{sp} \tag{2}$$

If this equation is applied, for example, at operation point 15, the fuel energy input per stroke for the diesel fuel is 1692.6 J/stroke, whereas the corresponding value for the B70 blend is 1689.6 J/stroke. Thus, the required fuel energy input per stroke to produce the same engine power are almost equal for the two alternative fuels. This implies also that the engine efficiency is not modified as a result of the shift to the biodiesel blend. The results of detailed calculations of engine efficiency for all operation points are included in Fig. 12 later.

The above remarks suggest that the engine is obliged to burn a higher B70 fuel quantity in order to produce the same torque at each operating point. The next step is to see whether this change in fuel quantity also affects A/F and λ. To this end, it must taken into account that a diesel engine is expected to draw approximately the same air quantity (mass) for a given engine speed and load. Since, as explained above, the engine needs to draw a higher fuel mass

per stroke to account for the lower energy content of B70, it is expected that A/F will be lower with the B70 fuel at all operating points. This is confirmed in Fig. 11. It must be noted here that A/F is measured by means of a UEGO sensor, which was originally calibrated for diesel fuel exhaust gas, which has $(A/F)_{st} = 14.5$. Stoichiometry calculations based on the above-mentioned methyl ester profile, produce a value for $(A/F)_{st}$ for our biodiesel sample of 12.48. This reduction in $(A/F)_{st}$ with respect to diesel fuel is mainly due to the oxygen content of the biodiesel molecules, and not to the difference in the C:H ratio, which remains approximately the same with biodiesel [**36**]. Based on this calculation, $(A/F)_{st}$ for the B70 mixture employed in these tests is estimated to be 13.08. The λ values shown in Fig. 11 ($\lambda = (A/F)/(A/F)_{st}$) are corrected according to this difference in $(A/F)_{st}$ between the two fuels.

According to this figure, A/F is reduced overall with the B70 biodiesel blend. On the other hand, λ is higher with the B70 blend for medium to high loads, whereas it is lower at low loads. As regards the exhaust gas temperature levels, they are reduced with the B70 blend in the medium-to-high load engine regime. A similar behaviour was reported in reference [**41**]. This fact deserves some additional discussion here. The differences in A/F should be partly related to the shifted operation points of the turbocharger, which affects exhaust temperature at turbine exit. It is interesting to see whether the engine draws the same levels of air mass flowrate in the case of the B70 fuel. The exhaust gas mass flowrate, calculated on the basis of the measured fuel flowrate and A/F, is also presented in Figure 11. The increase in fuel mass flowrate with B70 is accompanied by a decreased A/F with this blend. Overall, the exhaust gas mass flow rate is increased for medium to high loads. This implies that the turbocharger's operation point is shifted and this gives an explanation for the observed lower turbine out temperature.

The effect of biodiesel on the engine efficiency is another issue of interest here. A detailed calculation of engine efficiency was made according to

$$\eta_{th} = \frac{P}{\dot{m}_f H_u} = \frac{1}{\text{bsfc}\ H_u} \tag{3}$$

Fuel mass is calculated on the basis of fuel volume flowrate as measured by the ECU, taking into account the variable fuel density as a function of fuel temperature, as measured by the ECU. The results are employed in the calculation of bsfc and thermal efficiency values presented in Fig. 12.

To obtain the same torque and power output for both tested fuels, the bsfc was higher for the B70 blend in inverse proportion to the lower heating value per volume of fuel, leading to similar thermal efficiencies.

It should be mentioned here that the highest load selected for the comparison of the two fuels was less than the maximum torque. The reason for this selection lies in a certain reduction in the maximum torque that was observed with the B70 blend (240 N m instead of 250 N m). This reduction is explained by the fact that the maximum fuel delivery per stroke of about 55 mm^3/stroke in the engine's ECU maps (see Figs 2 to 6) does not suffice for the case of fuelling with B70 (Fig. 10) owing to its lower heating value.

Obviously, the ECU does not have the possibility of detecting the difference in fuel properties. In high-load conditions, the requirement by the accelerator of more torque increases the fuel delivery per stroke to the limits of the ECU's cartography. In order to keep the same maximum torque with biodiesel blends, an extension of the limits of the fuel delivery map would suffice, since an adequate margin of A/F exists. Moreover, if it became possible to trace the biodiesel percentage in the fuel by some kind of sensor, additional improvements would be possible in the ECU maps, to improve performance with the biodiesel blends further.

6.2 Effect of B70 fuel on the injection system parameters

The effect of B70 blend on the main fuel injection system parameters is presented in Fig. 13.

As shown in Fig. 13, the main injection advance and the pilot injection time were not affected by the use of the biodiesel blend. Thus, as expected for a common-rail fuel injection system [**8**, **9**], the difference in the speed of sound in biodiesel does not affect the start of the main injection (see Fig. 6). On the other hand, the rail pressure, pilot injection advance, and main injection time are increased with the B70 blend. This is explained by the algorithm of calculation of these variables by the ECU, altogether with the ECU cartography: the rail pressure is mapped in the ECU as a function of the engine speed and fuel delivery per stroke. Since biodiesel has a lower heating value than pure diesel, more fuel needs to be injected into the engine cylinder, which causes a higher fuel delivery and thus increased rail pressures (see Fig. 2) for the B70 fuel blend. The increase in pilot injection advance (see Fig. 5) and main injection time (see Fig. 3) were caused by the

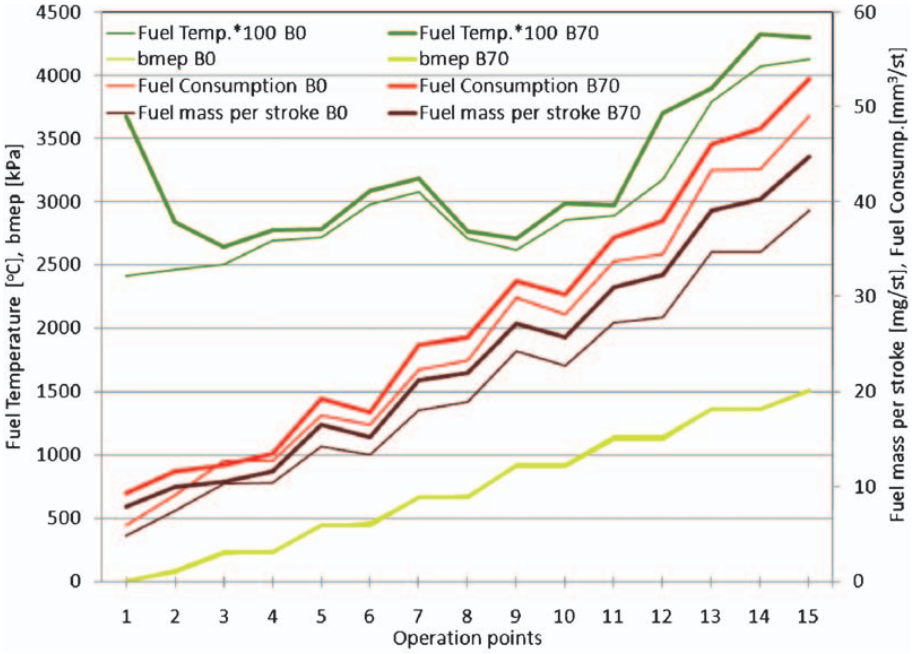

Fig. 10 Comparison of fuel delivery per stroke, fuel temperature, bmep and fuel mass per stroke for B0 and B70 at the 15 points of the cycle

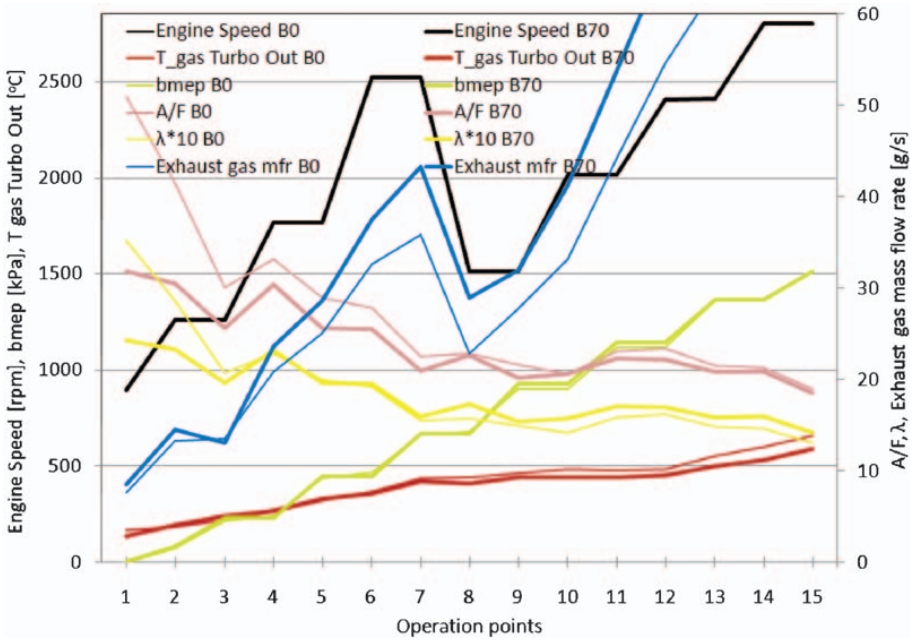

Fig. 11 Differences in A/F, λ, exhaust gas temperature, and mass flowrates at the 15 points of the cycle

effect of the increased fuel delivery, as calculated by the ECU based on the maps of Figs 2 to 6.

6.3 Effect of B70 on the pollutant emissions

The effect of the B70 fuel blend on the engine HC and CO emissions is presented in Fig. 14. The reduction in CO emissions is quite observable in the figure, especially at high loads. It is in line with the reported results of the literature. On the other hand, the effect of B70 fuel on THC emissions is less pronounced and is mainly seen at low to medium loads. Again, this is in line with what is reported in the literature for common-rail diesel engines [**28**].

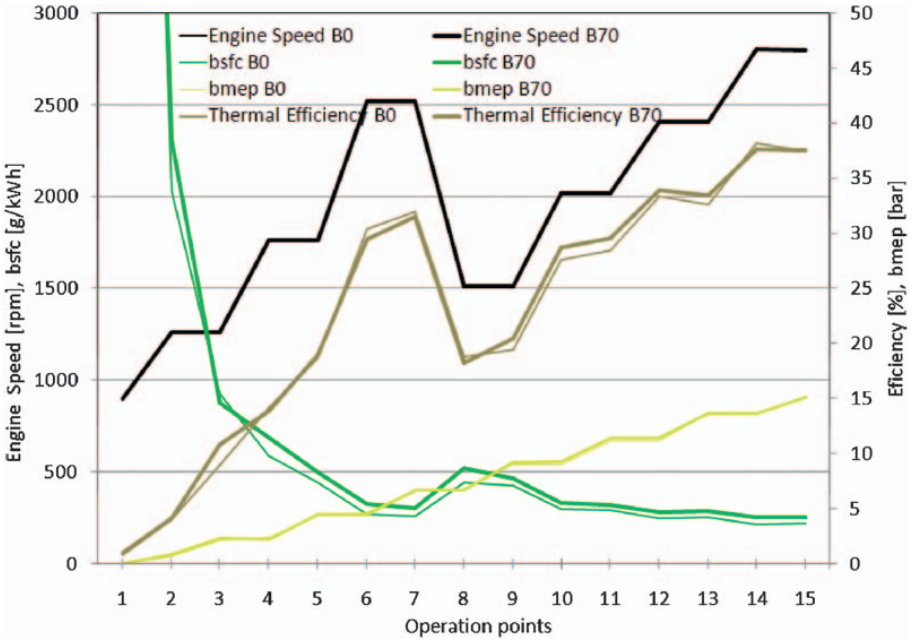

Fig. 12 Differences in bsfc, bmep, and engine efficiency at the 15 points of the cycle

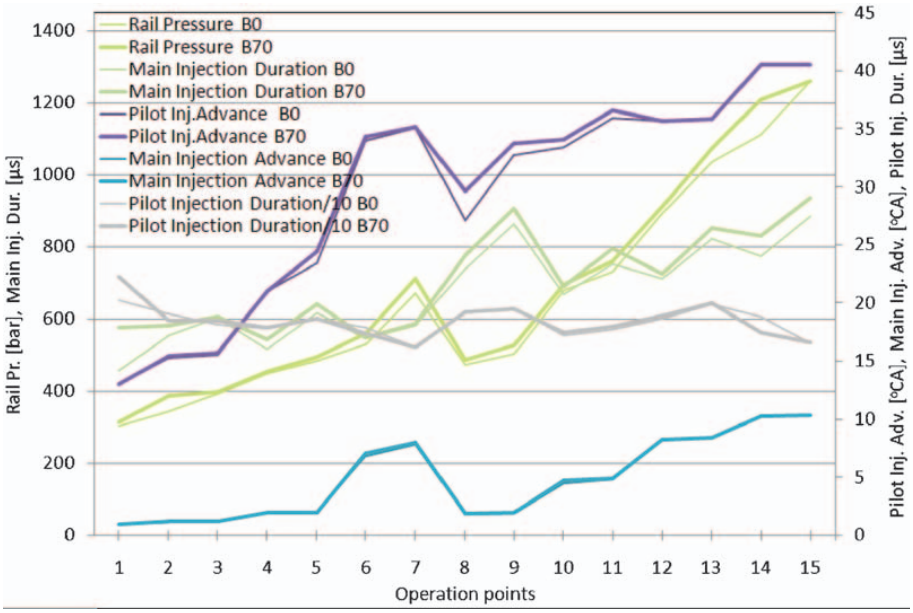

Fig. 13 Differences in fuel injection parameters (the common-rail pressure, pilot and main injection advance, and pilot and main injection duration) at the 15 points of the cycle

The effect of the B70 blend on the NO_x emissions is significantly more complicated, but again in line with what is reported in the literature [**7**, **42**, **43**]. According to the results presented in Fig. 15, there is a general trend of somewhat increased NO_x emissions in most part of the engine performance map. However, there exist certain operation points at medium to high engine loads, where NO_x emissions are reduced with the B70 blend. These points correspond to high-speed driving of the diesel-powered passenger car equipped with the specific engine. In Fig. 15, an attempt is made to correlate the observed variations in NO_x emissions with respective variation in fuel injection parameters and A/F. It can be seen that the operation points with increased NO_x emission with the B70 are generally characterized by a significant increase by the ECU of the pilot injection advance which points

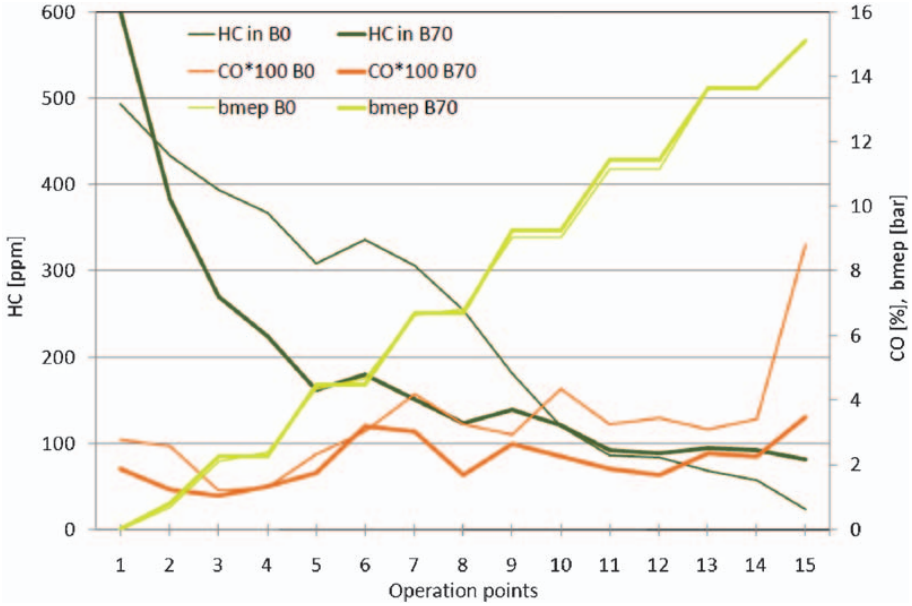

Fig. 14 Differences in HC and CO emissions between B70 and B0 at the 15 points of the cycle

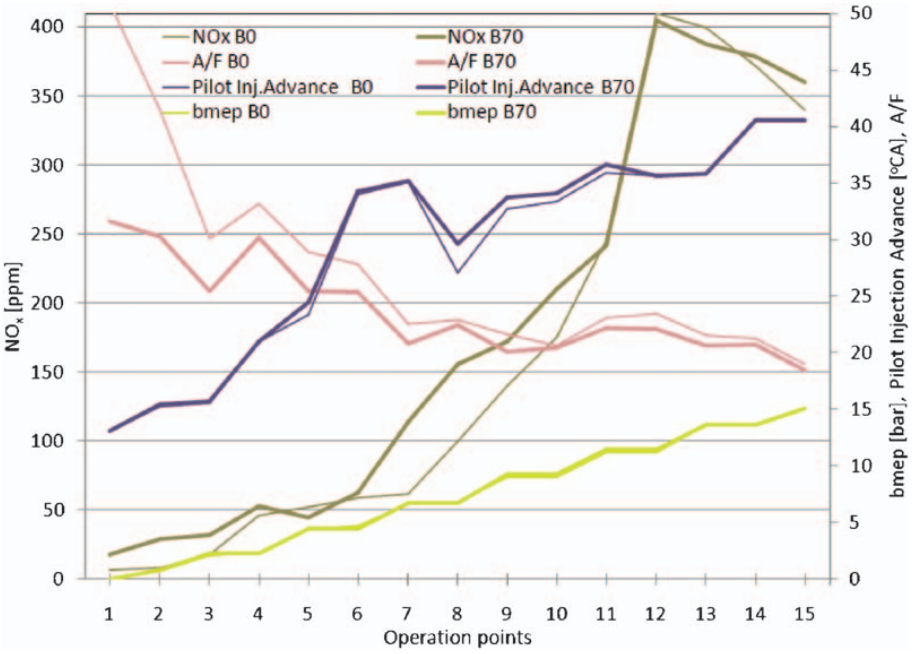

Fig. 15 Differences in NO_x emissions between B70 and B0 at the 15 points of the cycle

to an earlier start of combustion, in which case NO_x is expected to rise somewhat.

Finally, although the recorded particulate sampling was not carried out from diluted exhaust gas, the samples taken from undiluted gas very close to the exhaust line in 47 mm filters, one for each cycle, are comparatively presented in Fig. 16 just for a qualitative comparison. The lower blackening of the filter in the B70 case is apparent, altogether with the characteristic yellowish colour of the B70 particulate, which implies a higher SOF content. These observations, which are in accordance with the literature [**11**, **12**], can be mainly explained by the oxygen content of the biodiesel molecule, which enables more complete combustion and promotes the oxidation of the already-formed soot. In addition, the lower stoichiometric need for air in the case of biodiesel blend combustion reduces the probability of fuel-rich regions in the non-uniform fuel–air blend.

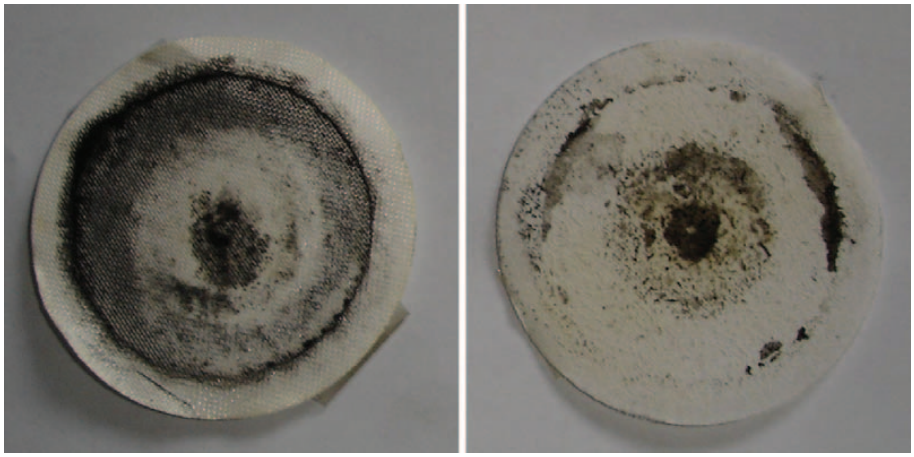

Fig. 16 Comparison of particulate samples (undiluted exhaust gas upstream filter passing through a Pallflex 47 mm filter during the total cycle): (a) diesel fuel; (b) B70 biodiesel blend

7 CONCLUSIONS

The specialized literature is relatively sparse regarding the effect of fuelling modern common-rail diesel engines by high-biodiesel-content fuel blends. This paper aims to contribute in this area by presenting comparative test results with a common-rail high-pressure injection passenger car diesel engine fuelled by B70 versus normal diesel fuel.

A sequence of 15 steady state engine operation points was selected as representative of the engine operation map. This test sequence was programmed in the controller of the eddy current dynamometer and the most important engine performance and emissions characteristics were recorded, with the engine fuelled by B70 and, alternatively, by pure diesel fuel.

The biodiesel employed in the tests was a FAME based on 40 per cent rapeseed oil, 30 per cent soybean oil and 30 per cent waste cooking oils as raw material, supplied by a local factory.

Engine tests performed under low-, medium- and high-load conditions have shown a sharp reduction in CO and HC emissions upstream of the catalyst, with the use of the B70 blend.

The effect of the decreased heating value of the biodiesel (despite its slightly increased density) in the bsfc increase was confirmed by the measurements. The Engine efficiency was not generally observed to change with biodiesel combustion.

As expected, decreased A/F values were measured with the B70 at all operation points. On the other hand, λ was observed to increase in the medium-load to high-load range.

The effect of the B70 blend on the main fuel injection parameters (the common-rail pressure, pilot and main injection advance, and time) was measured and explained on the basis of the maps stored in the ECU of the engine.

A significant increase in the fuel temperatures was observed with the B70 blend. It was necessary to install a heat exchanger in the fuel return line, in order to keep the fuel at acceptable temperatures (less than 50 °C).

The effect of the B70 on NO_x emissions was less pronounced and more complex. NO_x reduction was only observed at medium- to high-loads. Again, this can be explained on the basis of the modification by the ECU of certain fuel injection parameters for B70 combustion.

Reduced PM emissions and smoke opacity were observed by a qualitative comparison of the soot collected on Pallflex filters from undiluted exhaust gas sampled directly from the exhaust line for the total duration of each test. Again, this is in line with what is known from the literature.

The discussion improves understanding of how the common-rail injection engine responds to the biofuel blend, in comparison with the reference fuel, based on the injection control flow chart.

ACKNOWLEDGEMENTS

The financial support of the Hellenic General Secretariat of Research and Technology, in the framework of the collaborative project RIP A6 – Production of biofuels in Thessaly, is gratefully acknowledged. Also, the authors wish to thank the

local biodiesel production company ELIN biofuels SA for kindly supplying the quantity of biodiesel employed in the measurements free of charge.

REFERENCES

1 Biofuels in the European Union, a vision for 2030 and beyond, EUR 22066, final report of the Biofuels Research Advisory Council, 2007, available from http://ec.europa.eu/research/energy/pdf/biofuels_vision_2030_en.pdf.

2 European Biofuels Technology Platform, Strategic research agenda and strategic deployment document, 2008, available from http://cordis.europa.eu/technology-platforms/pdf/biofuels.pdf.

3 Fatty acid methyl esters fuels as a replacement or extender for diesel fuels, Diesel fuel injection equipment manufacturers common position statement, 2004, available from http://www.greenfuels.org/biodiesel/res/2004_10_FAME_Statement.pdf.

4 **Agarwal, A. K.** Biofuels (alcohols and biodiesel) applications as fuels for internal combustion engines. *Pro. Energy Combust. Sci.*, 2007, **33**(3), 233–271.

5 **Bouaid, A., Martinez, M.,** and **Aracil, J.** Production of biodiesel from bioethanol and Brassica carinata oil: Oxidation stability study. *Bioresource Technol.*, 2009, **100**(7), 2234–2239.

6 **Xin, J., Imahara, H.,** and **Saka, S.** Oxidation stability of biodiesel fuel as prepared by supercritical methanol. *Fuel*, 2008, **87**(10–11), 1807–1813.

7 **Graboski, M.** and **McCormick, R.** Combustion of fat and vegetable oil derived fuels in diesel engines. *Prog. Energy Combust. Sci.*, 1998, **24**, 125–164.

8 **Lapuerta, M., Armas, O.,** and **Rodriguez-Fernandez, J.** Effect of biodiesel fuels on diesel engine emissions. *Prog. Energy Combus. Sci.*, 2008, **34**(2), 198–223.

9 **McCormick, R. A. W. J. I. M. B. R. R. H.** Effects of biodiesel blends on vehicle emissions. Report, NREL/MP-540-40554, National Renewable Energy Laboratory, Golden Colorado, USA, 2006.

10 **Tsolakis, A., Megaritis, A., Wyszynski, M. L.,** and **Theinnoi, K.** Engine performance and emissions of a diesel engine operating on diesel-RME (rapeseed methyl ester) blends with EGR (exhaust gas recirculation). *Energy*, 2007, **32**(11), 2072–2080.

11 **Szybist, J. P., Song, J., Alam, M.,** and **Boehman, A. L.** Biodiesel combustion, emissions and emission control. *Fuel Processing Technol.*, 2007, **88**(7), 679–691.

12 **Wu, F., Wang, J., Chen, W.,** and **Shuai, S.** A study on emission performance of a diesel engine fueled with five typical methyl ester biodiesels. *Atmospheric Environment*, 2009, **43**(7), 1481–1485.

13 **Asad, U.** and **Zheng, M.** Fast heat release characterization of a diesel engine. *Int. J. Thermal Sci.*, 2008, **47**(12), 1688–1700.

14 **Renault,** DDCR diesel injection – fault finding – Diagnostics. In *(DDCR) DKDDCRI,* 2nd edition, 2007. 1

15 Directive 2003/30/EC of the European Parliament and of the Council of 8 May 2003 on the promotion of the use of biofuels or other renewable fuels for transport. *Off. J. Eur Union*, 2003, **L123**, 42–45.

16 A comprehensive analysis of biodiesel impacts on exhaust emissions. Report EPA 420-P-02-001, Assessment and Standards Division, Office of Transportation and Air Quality, US Environmental Protection Agency, Washington, DC, 2002.

17 Directive 98/69/EC of the European Parliament and of the Council relating to measures to be taken against air pollution by emissions from motor vehicles and amending Council Directive 70/220/EEC. *Off. J. Eur. Union*, 1998, **L350**, 1–57.

18 Proposal for a regulation of the European Parliament and of the Council on the type-approval of motor vehicles respect to emissions and on the access to vehicle repair information, amending Directive 72/306/EEC and Directive …/…/EC (EURO 6) (COM (2005) 683), 2005.

19 **Puhan, S., Vedaraman, N., Sankaranarayanan, G.,** and **Bharat, R. B.** Performance and emission study of Mahua oil (Madhuca indica oil) ethyl ester in a 4-stroke natural aspirated direct injection diesel engine. *Renewable Energy*, 2005, **30**, 1269–1278.

20 **Armas, O., Rodrıguez, J., Cardenas, M. D.,** and **Agudelp, A. F.** Efecto del biodiesel procedente de aceites vegetales usados sobre las emisiones y prestaciones de un motor diesel. In XVI Congreso Nacional de Ingeniería Mecánica, Leon, Spain, 2004. In *An. Ingeniería Mecánica*, 2004, **15**(3), 1739–1748.

21 **Lapuerta, M., Hernandez, J., Ballesteros, R.,** and **Duran, A.** Composition and size of diesel particulate emissions from a commercial European engine tested with present and future fuels. *Proc. Instn Mech. Engrs, Part D: J. Automobile Engineering*, 2003, **217**, 907–919.

22 **Lapuerta, M., Armas, O.,** and **Ballesteros, R.** Diesel particulate emissions from biofuels derived from Spanish vegetable oils. SAE paper 2002-01-1657, 2002.

23 **Cardone, M., Prati, M. V., Rocco, V.,** and **Senatore, A.** A comparative analysis of combustion process in D.I. diesel engine fueled with biodiesel and diesel fuel. SAE paper 2000-01-0691, 2000.

24 **Alam, M., Song, J., Acharya, R., Boehman, A.,** and **Muller, K.** Combustion and emissions performance of low sulfur, ultra low sulfur and biodiesel blends in a DI diesel engine. SAE paper 2004-01-3024, 2004.

25 **Szybist, J., Boehman, A., Taylor, J.,** and **McCormick, R.** Evaluation of formulation strategies to eliminate the biodiesel NO_x effect. *Fuel Proceesing Technol.*, 2005, **86**, 1109–1126.

26 **Boehman, A., Song, J.,** and **Alam, M.** Impact of biodiesel blending on diesel soot and the regenera-

tion of particulate filters. *Energy Fuels*, 2005, **19**, 1857–1864.
27 **Tat, M. E.** *Investigation of oxides of nitrogen emissions from biodiesel-fueled engines* (PhD Thesis, Iowa State University, Ames, Iowa, USA, 2003.
28 **Lapuerta, M., Herreros, J., Lyons, L., Garcia-Contreras, R.,** and **Briceno, Y.** Effect of the alcohol type used in the production of waste cooking oil biodiesel on diesel performance and emissions. *Fuel*, 2008, **87**(15–16), 3161–3169.
29 **Rodriguez-Anton, L. M., Aparicio, C., Guignon, B.,** and **Sanz, P. D.** Volumetric properties at high pressure of waste oil methyl ester compared with diesel oil. *Fuel*, 2008, **87**(10–11), 1934–1940.
30 **Leung, D. Y. C., Luo, Y.,** and **Chan, T. L.** Optimization of exhaust emissions of a diesel engine fuelled with biodiesel. *Energy Fuels*, 2006, **20**(3), 1015–1023.
31 **Yamane, K., Ueta, A.,** and **Shimamoto, Y.** Influence of physical and chemical properties of biodiesel fuels on injection, combustion and exhaust emission characteristics in a direct injection compression ignition engine. *Int. J. Engine Res.*, 2004, **4**, 249–261.
32 **Rakopoulos, C. D., Hountalas, D. T., Zannis, T. C.,** and **Levendis, Y. A.** Operational and environmental evaluation of diesel engines burning oxygen-enriched intake air or oxygen-enriched fuels: a review. SAE paper 2004-01-2924, 2004.
33 **Rakopoulos, D. C., Rakopoulos, C. D., Kakaras, E. C.,** and **Giakoumis, E. G.** Effects of ethanol-diesel fuel blends on the performance and exhaust emissions of heavy duty DI diesel engine. *Energy Conversion Managmt*, 2008, **49**(11), 3155–3162.
34 EN 14214: 2003 Fatty acid methyl esters (FAME) for diesel engines – requirements and test methods, 2003 (European Committee for Standardization, Brussels).
35 **Jääskeläinen, H.** Biodiesel standards and properties, 2007, available from www.dieselnet.com.
36 DieselNet, Appendix: biodiesel composition and properties of components, 2007, available from www.dieselnet.com.
37 **Knothe, G.** 'Designer' biodiesel: optimizing fatty ester composition to improve fuel properties. *Fuel*, 2008, **22**, 1358–1364.
38 **Demetriades, L., Tziourtzioumis, D., Zogou, O.,** and **Stametelos, A. M.** RIP A6 – production of biofuels in Thessaly: engine tests with biodiesel mixtures, Volos. Report (Contract RIP A6: Document 2), 2008.
39 **Castellon-Elizondo, E., Lutz, G.,** and **Mata-Segreda, G.** The soft-solid model for liquids. Application to biodiesel and other materials of technological interest. *Phys. Org. Chemistry*, 2006, **19**, 744–747.
40 *VDI-Wärmeatlas*, 2002 (Springer Verlag, Berlin).
41 **Kegl, B.** Effects of biodiesel on emissions of a bus diesel. *Bioresource Technol.*, 2007, **99**(4), 863–873.
42 **Knothe, G., Matheaus, A.,** and **Ryan, T. W.** Cetane numbers of branched and straight-chain fatty esters determined in an ignition quality tester. *Fuel*, 2003, **82**(8), 971–975.
43 **Murphy, M., Taylor, J.,** and **McCormick, R.** Compendium of experimental cetane number data. Report NREL/SR-540-36805, National Penetrable Energy Laboratory, Golden, Colorado, USA, 2004.

APPENDIX

Notation

A/F	Air-to-fuel ratio
$(A/F)_{st}$	stoichiometric air-to-fuel ratio
bmep	brake mean effective pressure (bar)
bsfc	brake specific fuel consumption (g/kW h)
b_{sp}	fuel delivery per stroke (fuel consumption) (mm^3/stroke)
CA	crank angle (degp)
ECU	electronic control unit
E_{str}	fuel energy input per stroke (J/stroke)
FAME	fatty acid methyl ester
H_u	gross heating value (MJ/kg]
mfr	mass flowrate (kg/s)
m_f	fuel mass flowrate (kg/s)
PM	particulate matter
P	engine power (kW)
UEGO	universal exhaust gas oxygen (sensor)
β	coefficient of volume thermal expansion (K^{-1})
η_{th}	thermal efficiency (per cent)
λ	$= (A/F)/(A/F)_{st}$
ρ_f	fuel density (kg/m^3)
ρ_0	density at 15 °C (kg/m^3)